View metadata, citation and similar papers at core.ac.uk
brought to you by CORE
provided by Elsevier - Publisher Connector

Cell

Epiblast Stem Cell Subpopulations Represent Mouse Embryos of Distinct Pregastrulation Stages

Dong Wook Han,[1] Natalia Tapia,[1] Jin Young Joo,[1] Boris Greber,[1] Marcos J. Araúzo-Bravo,[1] Christof Bernemann,[1] Kinarm Ko,[2,3] Guangming Wu,[1] Martin Stehling,[1] Jeong Tae Do,[4] and Hans R. Schöler[1,5,*]
[1]Department of Cell and Developmental Biology, Max Planck Institute for Molecular Biomedicine, Röntgenstrasse 20, 48149 Münster, Germany
[2]Center for Stem Cell Research, Institute of Biomedical Sciences and Technology
[3]Department of Neuroscience, School of Medicine
Konkuk University, Hwayang-dong, Gwangjin-gu, Seoul 143-701, Republic of Korea
[4]Laboratory of Stem Cell and Developmental Biology, CHA Stem Cell Institute, CHA University, 605-21 Yoeksam 1-dong, Gangnam-gu, Seoul 135-081, Republic of Korea
[5]University of Münster, Medical Faculty, Domagkstrasse 3, 48149 Münster, Germany
*Correspondence: office@mpi-muenster.mpg.de
DOI 10.1016/j.cell.2010.10.015

SUMMARY

Embryonic stem cells (ESCs) comprise at least two populations of cells with divergent states of pluripotency. Here, we show that epiblast stem cells (EpiSCs) also comprise two distinct cell populations that can be distinguished by the expression of a specific *Oct4*-GFP marker. These two subpopulations, *Oct4*-GFP positive and negative EpiSCs, are capable of converting into each other in vitro. *Oct4*-GFP positive and negative EpiSCs are distinct from ESCs with respect to global gene expression pattern, epigenetic profile, and *Oct4* enhancer utilization. *Oct4*-GFP negative cells share features with cells of the late mouse epiblast and cannot form chimeras. However, *Oct4*-GFP positive EpiSCs, which only represent a minor EpiSC fraction, resemble cells of the early epiblast and can readily contribute to chimeras. Our findings suggest that the rare ability of EpiSCs to contribute to chimeras is due to the presence of the minor EpiSC fraction representing the early epiblast.

INTRODUCTION

Four different types of pluripotent stem cells have been established in culture to date: EC (embryonal carcinoma) cells from teratocarcinomas, ES (embryonic stem) cells from the inner cell mass (ICM), EG (embryonic germ) cells from PGCs (primordial germ cells), and EpiSCs (epiblast stem cells) from developing epiblasts (Lovell-Badge, 2007). ES, EC, and EG cells are capable of efficiently forming both teratomas and chimeras. However, although EpiSCs readily form teratomas, they rarely form chimeras (Brons et al., 2007; Tesar et al., 2007). This feature suggests that EpiSCs may exhibit restricted pluripotency relative to other pluripotent stem cells despite similarities in gene expression and epigenetic profile (Chou et al., 2008). To our knowledge, EpiSCs represent only one cell type exhibiting this restricted potency. This limited potency of EpiSCs may be inherent to the tissue of origin or newly arises from the different culture environment of EpiSCs compared with ES cells (ESCs). This latter possibility is corroborated by evidence indicating that mouse ESCs require LIF and BMP4 to maintain pluripotency (Ying et al., 2003), whereas EpiSCs require bFGF and Activin A (Brons et al., 2007; Tesar et al., 2007). The low potency of EpiSCs can also be explained by the inability of these cells to grow and survive as single cells when injected into a blastocyst, preventing them from incorporating into the ICM. Another possible explanation concerns the developmental stage gap of the cells involved—donor EpiSCs are of embryonic day 5.5 (E5.5) to ~E7.5, whereas recipient blastocysts are of E3.5. However, these possible explanations do not fully explain the distinct pluripotency of EpiSCs. A final explanation may be that EpiSCs are actually heterogeneous in nature and thus comprise at least two distinct subpopulations, one with higher developing potency and the other with lower potency, possibly accounting for the apparent discrepancy in the potency of EpiSCs observed with different in vivo development assays.

ESCs have long been considered to represent a homogeneous population of cells; however, recent studies based on *Stella* (*Dppa3*) and *Rex1* (*Zfp42*) expression have demonstrated that ESCs comprise a heterogeneous cell population (Hayashi et al., 2008; Toyooka et al., 2008). Different cell subpopulations represent different in vivo developmental stages, with a dynamic interchange between cells of an ICM-like state and those of an epiblast- or primitive ectoderm-like state. Similarly, ESC expression levels of stage-specific embryonic antigen 1 (SSEA1) and platelet endothelial cell adhesion molecule 1 (Pecam1) have been shown to correlate with ESC pluripotency (Furusawa et al., 2004). Strikingly, intermittent *Nanog* expression has

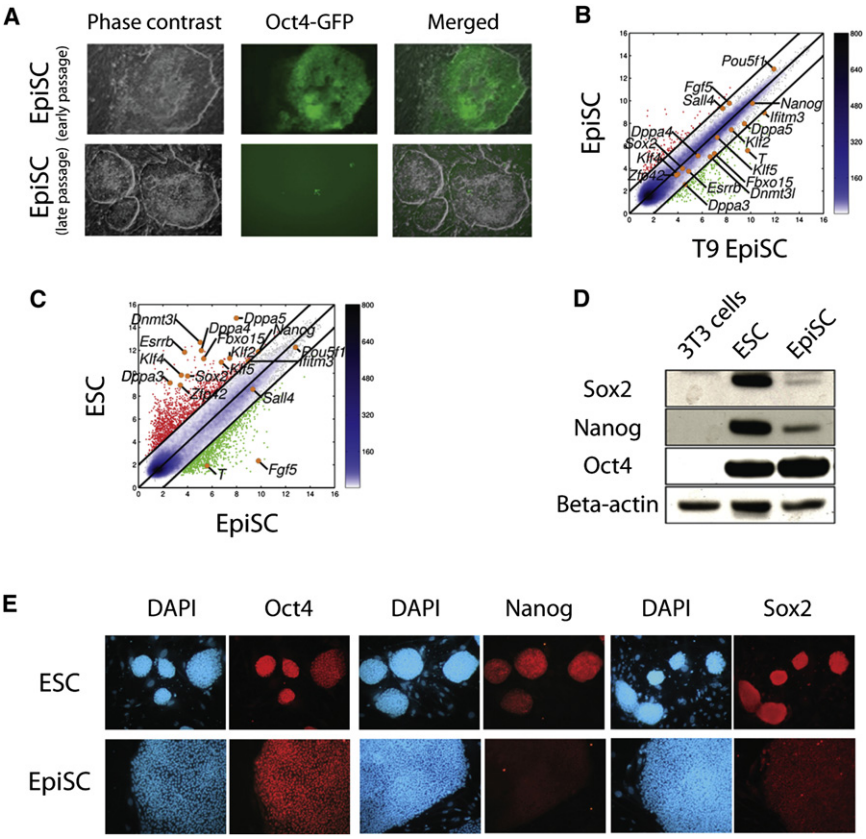

Figure 1. Characterization of GOF18 EpiSCs

(A) Morphology and *Oct4*-GFP expression in the established GOF18 EpiSC line at early and late passages.

(B and C) Scatter plots of global gene expression microarrays comparing GOF18 EpiSCs with T9 EpiSCs (B) and ESCs (C). The black lines delineate the boundaries of 2-fold difference in gene expression levels. Genes highly expressed in ordinate samples compared with abscissas samples are shown as green circles; those less expressed are shown as red. Positions of pluripotent cell (*Pou5f1*/*Oct4*, *Sox2*, *Nanog*, *Klf2*, *Klf4*, *Klf5*, *Sall4*, *Dnmt3l*, *Esrrb*, *Fbxo15*, and *Zfp42*/*Rex1*), germ cell (*Stella [Dppa3]*, *Dppa4*, *Dppa5*, *Ifitm3 [Fragilis]*), and epiblast (*Fgf5*, *T*) markers are indicated with orange dots. The color bar to the right indicates the scattering density; the higher the scattering density, the darker the blue color. Gene expression levels are depicted on $\log_2$ scale.

(D) Protein levels of pluripotency markers in EpiSCs. Levels of Oct4, Nanog, and Sox2 were compared in ESCs and EpiSCs by western blot; 3T3 cells were used as a negative control.

(E) Immunofluorescence analysis for Oct4, Nanog, and Sox2 in ESCs and EpiSCs. DAPI was used for nuclear staining.

been associated with distinct functional ESC phenotypes (Chambers et al., 2007). Thus, undifferentiated ESC cultures comprise cells of different pluripotency levels corresponding to different developmental stages in the embryo. To date, EpiSCs have been considered to represent a homogeneous pluripotent cell population due to their high methylation compared with ESCs. This epigenetic profile may result in reduced EpiSC plasticity, thus preventing cellular heterogeneity, as observed in ESCs (Hayashi et al., 2008; Toyooka et al., 2008).

Primitive ectoderm (PrE) cells of developing epiblasts have been generally described to be incapable of contributing to chimera formation, although they still retain differentiation potential and can give rise to cells of all three germ layers (Gardner et al., 1985; Lawson et al., 1991; Tesar et al., 2007). However, Gardner et al. demonstrated that PrE cells from an early stage, such as E5, still have the capability for chimeric contribution, but they lose it within the next 24 hr (Gardner et al., 1985). Therefore, if we consider the developing potency of early-stage epiblasts and the heterogeneity of ESCs, we can surmise that EpiSCs may comprise a heterogeneous population, like ESCs, and that a minor or rare subpopulation of EpiSCs exists that contributes to chimera formation, with the major EpiSC subpopulation having no such developing potency, like late-stage epiblasts.

In this study, we explored the distinct pluripotential state of EpiSCs by investigating the homogeneity of EpiSCs in culture. Based on the distinct expression of an *Oct4*-GFP transgene, we found that EpiSCs are not homogeneous but, rather, comprise two distinct cell subpopulations: an *Oct4*-GFP positive population and an *Oct4*-GFP negative population. These two subpopulations displayed clear differences in molecular characteristics and developmental potential, including capability for chimera formation. We show that these two subpopulations do not represent spontaneously converted ES-like cells but, rather, resemble cells of early- and late-stage postimplantation embryos. Therefore, our findings suggest that the observed discrepancy in a pluripotential capacity of EpiSCs (teratoma versus chimera formation) is due to the presence of two functionally distinct subpopulations of EpiSCs in culture.

RESULTS

Dynamic Expression of an *Oct4*-GFP Transgene in Established GOF18 EpiSCs

Epiblast stem cells were derived from GOF18 (genomic *Oct4* fragment, 18 kb) mice containing a GFP transgene under the control of the entire regulatory region of the *Oct4* gene (Yeom et al., 1996). A characteristic feature of mouse EpiSCs is the preferential use of the proximal enhancer (PE) over the distal enhancer (DE) for *Oct4* gene transcription (Tesar et al., 2007). Thus, both established EpiSCs from GOF18 mice and postimplantation epiblasts should theoretically express *Oct4* and be *Oct4*-GFP positive. We first examined the expression of *Oct4*-GFP in both established EpiSCs (Figure 1A) and postimplantation epiblasts (Figure 5E). Whereas the in vivo epiblast was

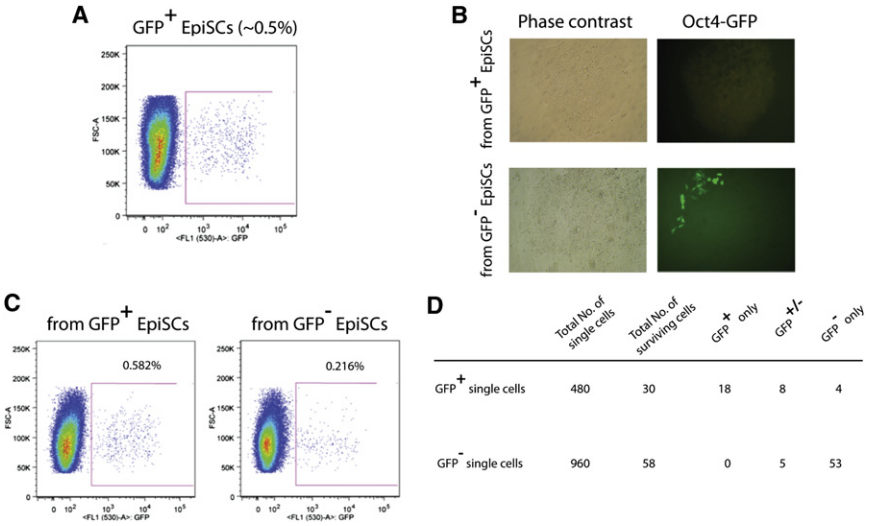

Figure 2. Dynamic Expression of *Oct4*-GFP in GOF18 EpiSCs

(A) Percentage of *Oct4*-GFP positive cells in EpiSCs measured by FACS sorting.

(B) *Oct4*-GFP positive and *Oct4*-GFP negative EpiSCs were FACS sorted and cultured separately. An *Oct4*-GFP negative colony from *Oct4*-GFP positive cells and an *Oct4*-GFP positive colony from *Oct4*-GFP negative cells observed under fluorescence microscope after 1 week in culture are shown.

(C) Percentage of *Oct4*-GFP positive cells from both *Oct4*-GFP positive and *Oct4*-GFP negative cells was measured by FACS 7 days after the initial sorting.

(D) Summary of the clonal assay. FACS-sorted *Oct4*-GFP positive and negative single cells were plated on 96-well plates, and *Oct4*-GFP expression was monitored under fluorescence microscope during 1 week. The numbers of clonal cell lines containing only GFP positive cells, only GFP negative cells, or a mixture of GFP positive and negative cells are indicated.

Oct4-GFP positive, only a very low percentage of established GOF18 EpiSCs retained *Oct4*-GFP expression after a few passages (Figure 1A and Figure 2A; see also Figure 5E).

GOF18 EpiSCs exhibited a global gene expression profile very similar to that of an independently derived EpiSC line but distinct from that of ESCs, confirming that GOF18 cells are bona fide EpiSCs (Tesar et al., 2007) (Figures 1B and 1C). Oct4 protein levels were similar in ESCs and EpiSCs, but Sox2 and Nanog protein levels were lower in EpiSCs (Figures 1D and 1E), consistent with published data (Silva et al., 2009).

Therefore, the expression of the *Oct4*-GFP transgene did not appear to correspond to that of the endogenous *Oct4* gene in GOF18 EpiSCs, prompting us to speculate that this may be due to an adaptation of the in vivo epiblast to the in vitro culture conditions. Similarly, the ICM undergoes adaptive modifications during the establishment of ESCs, as previously described (Buehr and Smith, 2003; Rossant, 2001). Thus, inactivation of the *Oct4*-GFP transgene might actually result from epigenetic modifications occurring in the in vitro culture—a change that may affect the GFP transgene, but not the endogenous *Oct4* locus at the gene and protein levels. However, ~0.5% of GOF18 EpiSCs remained *Oct4*-GFP positive after serial passages (Figure 2A).

Next, we sought to investigate the characteristics of this *Oct4*-GFP positive population of EpiSCs. To this end, we sorted *Oct4*-GFP positive and negative cells by fluorescence-activated cell sorting (FACS) and cultured them separately. Of interest, 48 hr after FACS sorting, *Oct4*-GFP positive cells started to lose GFP expression. On the other hand, some *Oct4*-GFP negative cells started to gain GFP expression (Figure 2B). After 1 week in culture, the percentage of *Oct4*-GFP positive cells in each culture was similar to that of the parental nonsorted EpiSCs. *Oct4*-GFP negative EpiSCs gave rise to a small proportion of *Oct4*-GFP positive EpiSCs (~0.2% *Oct4*-GFP positive), whereas the majority of *Oct4*-GFP positive EpiSCs converted to *Oct4*-GFP negative EpiSCs (~0.5% *Oct4*-GFP positive) (Figure 2C). To better characterize this conversion, we performed a clonal assay (Figure 2D). We then FACS sorted single *Oct4*-GFP positive and negative cells in 96-well plates (10 × 96-well plates with *Oct4*-GFP negative EpiSCs and 5 × 96-well plates with *Oct4*-GFP positive EpiSCs). Fifty-eight of 960 *Oct4*-GFP negative EpiSCs and 30 of 480 *Oct4*-GFP positive EpiSCs had survived after 1 day in culture. After 1 week in culture, five *Oct4*-GFP negative clonal lines showed partial reactivation of the *Oct4*-GFP transgene. Similarly, 12 *Oct4*-GFP positive single cell lines lost *Oct4*-GFP expression—either partially or entirely (Figure 2D). These results indicated that both *Oct4*-GFP positive and negative EpiSCs had the ability to interconvert, resulting in a state of dynamic equilibrium between *Oct4*-GFP positive and negative EpiSCs in culture.

Oct4-GFP Positive and Negative EpiSCs Have Distinct Gene Expression Profiles

Next, we assessed whether the *Oct4*-GFP positive and negative subpopulations differ at the molecular level. The global gene expression profile of both FACS-sorted subpopulations was determined by microarray analysis. The global gene expression profile of *Oct4*-GFP negative EpiSCs, which represented ~99% of the entire GOF18 EpiSC culture, matched that of the parental nonsorted GOF18 EpiSCs (Figure 3A). Moreover, the global expression profile of the *Oct4*-GFP positive fraction was very similar to that of the negative fraction, but both differed markedly from that of an ESC control transcriptome (Figures 3A and 3B). In other words, both EpiSC subpopulations indeed constitute EpiSCs and not, for example, spontaneously converted ES-like cells. ESC marker genes, such as *Klf2*, *Klf4*, *Dnmt3l*, *Esrrb*, *Stella* (*Dppa3*), *Fbxo15*, *Rex1* (*Zfp42*), and *Dppa5*, were upregulated in the *Oct4*-GFP positive subpopulation compared with the *Oct4*-GFP negative fraction (Figure 3A and Figure S1 available online). Similarly, EpiSC markers, such as *Fgf5* and *Brachyury* (*T*), were downregulated in GFP positive subpopulation compared with negative EpiSCs. Overall, these findings indicate that *Oct4*-GFP

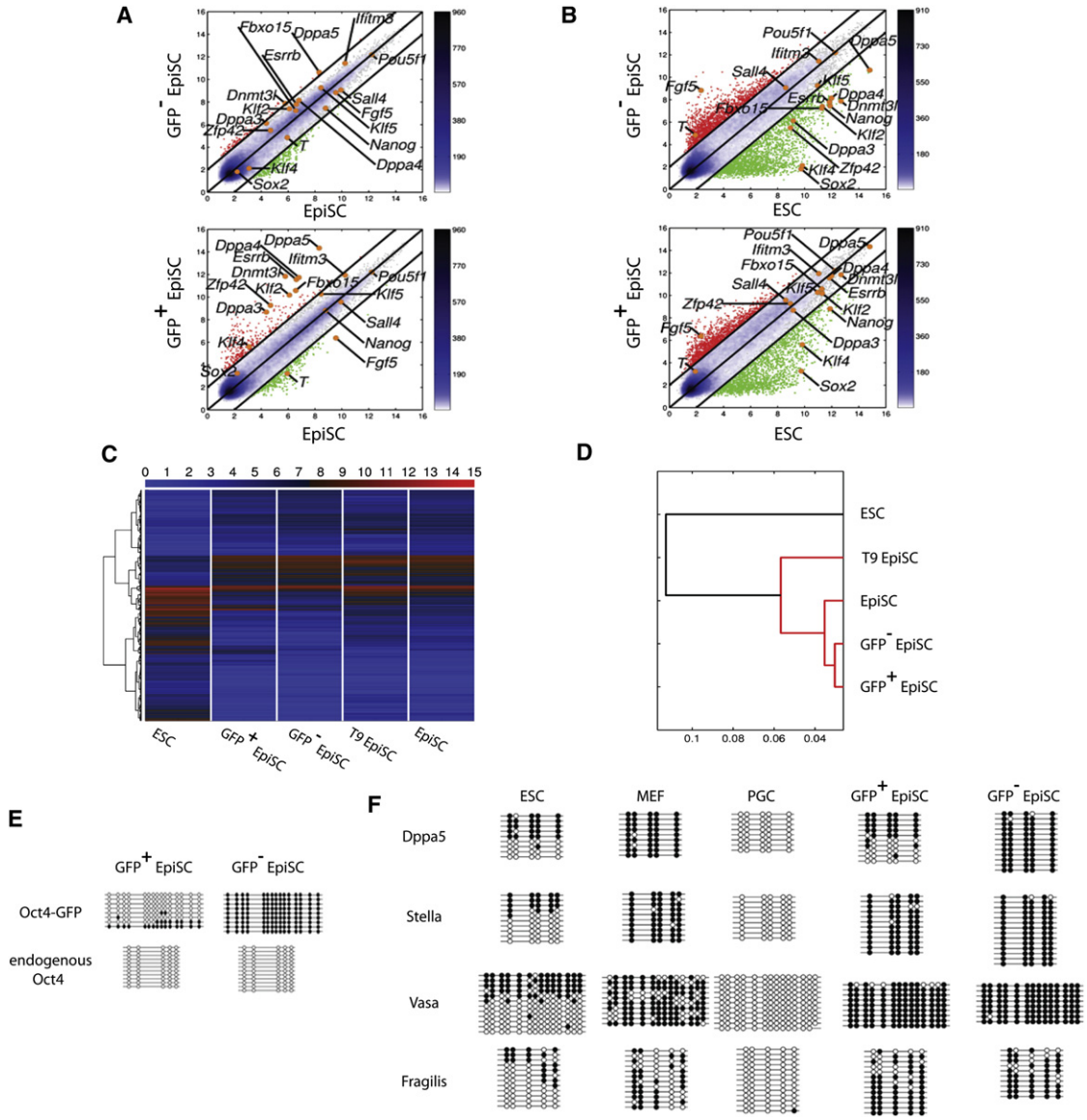

Figure 3. *Oct4*-GFP Positive and Negative EpiSCs Have Distinct Gene Expression and Epigenetic Profiles

(A) Scatter plots of global gene expression microarray comparing *Oct4*-GFP negative and positive EpiSCs with nonsorted EpiSCs.

(B) Scatter plots of global gene expression microarrays comparing *Oct4*-GFP negative and positive EpiSCs with ESCs. The black lines delineate the boundaries of 2-fold difference in gene expression levels. Genes highly expressed in ordinate samples compared with abscissas samples are shown as green circles; those less expressed are shown as red. Positions of pluripotent cell (*Pou5f1*/*Oct4*, *Sox2*, *Nanog*, *Klf2*, *Klf4*, *Klf5*, *Sall4*, *Dnmt3l*, *Esrrb*, *Fbxo15*, and *Zfp42*/*Rex1*), germ cell (*Stella [Dppa3]*, *Dppa4*, *Dppa5*, *Ifitm3 [Fragilis]*), and epiblast (*Fgf5*, *T*) markers are indicated with orange dots. The color bar to the right indicates the scattering density; the higher the scattering density, the darker the blue color. Gene expression levels are depicted on $\log_2$ scale.

(C) Heat map of global gene expression patterns in ESCs, *Oct4*-GFP positive and negative EpiSCs, T9 EpiSCs, and GOF18 EpiSCs. The color bar at top codifies the gene expression in $\log_2$ scale. Red and blue colors indicate high and low gene expression, respectively.

(D) Hierarchical clustering shows that *Oct4*-GFP positive EpiSCs clustered close to the parental EpiSCs or T9 EpiSCs, but not to ESCs.

(E) DNA methylation status of the promoter regions of both the endogenous *Oct4* gene and the *Oct4*-GFP transgene was determined by bisulfite sequencing PCR.

(F) *Dppa5*, *Stella* (*Dppa3*), *Vasa*, and *Fragilis* (*Ifitm3*) promoter regions were analyzed by bisulfite sequencing PCR in ESCs, MEFs, and PGCs, as well as in *Oct4*-GFP positive and negative EpiSCs.

See also Figure S1.

positive cells were still EpiSCs by identity, but they differed from the more abundant EpiSC subpopulation by the expression of several prominent marker genes.

Recent reports have described that EpiSCs are capable of converting to an ES-like state under specific culture conditions (Bao et al., 2009; Greber et al., 2010; Guo et al., 2009; Hanna

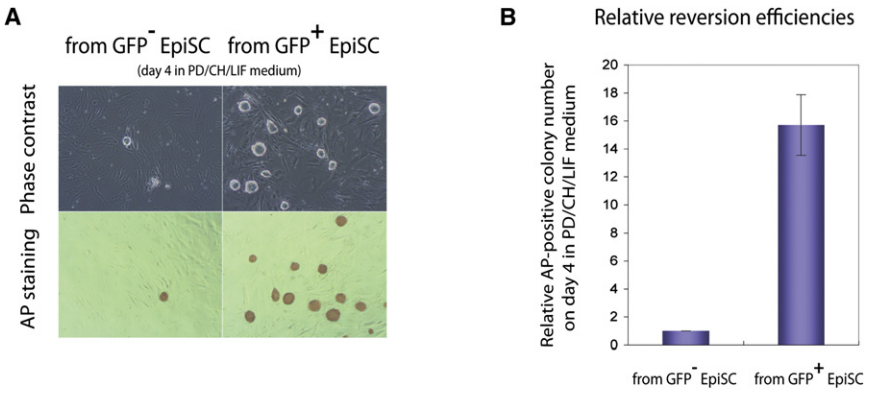

Figure 4. *Oct4*-GFP Positive and Negative EpiSCs Show Distinct ESC Conversion Efficiency

(A) Conversion of both the *Oct4*-GFP positive and negative EpiSCs to an ES-like cell state using a conversion condition (2i+LIF). Morphology and alkaline phosphatase (AP) activity of EpiSCs after 4 days of treatment are shown.

(B) Relative conversion efficiency of *Oct4*-GFP positive and negative EpiSCs was determined by counting the number of AP-positive colonies. Data represent mean ± SEM of triplicates; n = 3.

(C) *Dppa5*, *Stella*, *Vasa*, and *Fragilis* promoter regions in the converted ES-like cells were analyzed by bisulfite sequencing PCR.

See also Figure S2.

et al., 2009). We therefore sought to further rule out the possibility that *Oct4*-GFP positive EpiSCs represented EpiSCs that had converted to an ES-like state. As revealed by hierarchical clustering, *Oct4*-GFP positive as well as *Oct4*-GFP negative EpiSCs clearly differed from ESCs and clustered with an independent EpiSC line (Figures 3C and 3D). Thus, the *Oct4*-GFP positive EpiSC subpopulation did not represent EpiSC cells that had spontaneously converted to an ES-like state.

Epigenetic Differences between *Oct4*-GFP Positive and Negative EpiSCs

We then asked whether at least some of the differences in gene expression between *Oct4*-GFP positive and negative EpiSCs (Figure 3A) could have resulted from differential epigenetic modifications. To this end, we determined the DNA methylation status of the endogenous and transgenic *Oct4* loci in both *Oct4*-GFP positive and negative EpiSCs. Consistent with the gene expression profiling data (Figure 3A), the promoter regions of endogenous *Oct4* were completely unmethylated in both subpopulations (Figure 3E). However, the *Oct4*-GFP transgene promoter was hypomethylated in *Oct4*-GFP positive EpiSCs but highly methylated in *Oct4*-GFP negative EpiSCs (Figure 3E). These data indicate that the mechanism regulating the dynamic *Oct4*-GFP fluctuations in EpiSC culture is related to the differential DNA methylation status of the *Oct4*-GFP promoter in *Oct4*-GFP positive and negative EpiSCs.

Next, we assessed whether *Oct4*-GFP positive cells may represent early PGCs. To this end, we examined the promoter regions of the germ cell markers *Stella* (*Dppa3*), *Vasa*, and *Fragilis* (*Ifitm3*) in ESCs, *Oct4*-GFP positive as well as negative EpiSCs, PGCs, and mouse embryonic fibroblasts (MEFs). As expected, all promoter regions examined were fully methylated in MEFs but completely unmethylated in PGCs. All of these genes exhibited an imprinted methylation pattern in ESCs, which is due to the heterogeneous expression of many germ cell markers (Carter et al., 2008). In contrast, germ cell marker genes were fully methylated in *Oct4*-GFP negative as well as the positive EpiSCs, like in MEFs, but not in ESCs or PGCs (Figure 3F). Finally, parental nonsorted EpiSCs exhibited the same methylation pattern as *Oct4*-GFP negative EpiSCs (data not shown). These data further support the notion that *Oct4*-GFP positive cells have an overall EpiSC identity that is neither ES-like nor PGC-like.

In contrast, the methylation pattern of the *Dppa5* promoter was similar in *Oct4*-GFP positive EpiSCs and ESCs (Figure 3F). This is consistent with the gene expression profiling data, revealing increased *Dppa5* expression in *Oct4*-GFP positive EpiSCs compared with *Oct4*-GFP negative EpiSCs (Figure 3A). These data suggest that *Oct4*-GFP positive cells differ from *Oct4*-GFP negative cells in the expression of some prominent ESC marker genes, as reflected by differential epigenetic regulation. These data further suggest that the dynamic interchange between the *Oct4*-GFP positive and negative subpopulations of EpiSCs appears to be regulated by a DNA methylation-dependent mechanism.

Oct4-GFP Positive and Negative EpiSCs Show Distinct ESC Conversion Rates

Next, we asked whether these two EpiSC populations differ in function. EpiSCs can be converted to an ES-like state by switching to stringent ESC culture conditions, the so-called 2i+LIF medium (2i condition) (Greber et al., 2010; Guo et al., 2009; Hanna et al., 2009). As *Oct4*-GFP positive cells exhibited upregulation of some prominent ESC markers, we speculated that *Oct4*-GFP positive EpiSCs can be converted more easily than *Oct4*-GFP negative EpiSCs. Under the 2i condition, the conversion efficiency of *Oct4*-GFP positive EpiSCs was much higher compared with that of *Oct4*-GFP negative EpiSCs, as determined by the number of colonies staining positive for alkaline phosphatase (Figures 4A and 4B). Remarkably, conversion of

Oct4-GFP positive EpiSCs was noted only in the presence of 2i+LIF, and not in EpiSC medium. Consistent with a previous study (Bao et al., 2009), we also obtained converted ES-like cells in typical ESC medium (LIF alone). However, we were unable to maintain these converted cells with LIF alone (data not shown). Thus, although *Oct4*-GFP positive cells do not represent ES-like cells, they can be converted at substantially higher efficiency than *Oct4*-GFP negative EpiSCs.

Finally, to definitively rule out the possibility that *Oct4*-GFP positive EpiSCs are actually spontaneously converted ES-like cells, we assessed the promoter methylation patterns of *Stella*, *Fragilis*, *Vasa*, and *Dppa5* in the ES-like cells that had been converted from *Oct4*-GFP positive EpiSCs. The *Stella* promoter is known to be differentially methylated in EpiSCs and ESCs (Bao et al., 2009; Hayashi et al., 2008). As shown in Figure 4C, the converted ES-like cells exhibited an imprinted DNA methylation pattern of the *Stella* promoter, like ESCs, but a clearly different pattern compared with *Oct4*-GFP positive EpiSCs, from which they had been derived (Figure 3F). Similarly, the converted ES-like cells exhibited hypomethylation of the *Rex1* promoter region, but both *Oct4*-GFP positive and negative EpiSCs showed high *Rex1* promoter methylation (Figure S2). Moreover, the converted ES-like cells also showed reduced DNA promoter methylation of the germ cell markers *Fragilis*, *Vasa*, and *Dppa5*, like ESCs, whereas *Oct4*-GFP positive EpiSCs exhibited hypermethylation of these germ cell marker genes (Figure 4C and Figure 3F). Therefore, the distinct DNA methylation pattern in *Oct4*-GFP positive EpiSCs and converted ES-like cells allows us to definitively rule out that the *Oct4*-GFP positive EpiSC subpopulation represents EpiSCs that had spontaneously converted to an ES-like state in EpiSC culture.

Oct4-GFP Positive and Negative EpiSCs Represent Pregastrulation Epiblasts of Different Developmental Stages

Oct4-GFP positive and *Oct4*-GFP negative EpiSCs exhibit differential expression of some ESC marker genes (Figure 3A), distinguishable *Dppa5* methylation pattern (Figure 3F), and distinct ESC conversion efficiency (Figures 4A and 4B). Of interest, *Dppa5*, which was less methylated in *Oct4*-GFP positive than in *Oct4*-GFP negative EpiSCs (Figure 3F), is expressed in E5.5 epiblasts, but not in E6.5 epiblasts (Western et al., 2005). On the other hand, the typical EpiSC marker *T*, which was highly expressed in *Oct4*-GFP negative compared with *Oct4*-GFP positive EpiSCs, is more abundant in E6.5 epiblasts than in E5.5 epiblasts (Rivera-Pérez and Magnuson, 2005). These observations prompted us to investigate whether the cells with different *Oct4*-GFP transgene expression actually correspond to in vivo epiblasts of different developmental stages. For this purpose, we compared the gene expression profiles of E5.5 and E6.5 in vivo epiblasts isolated from GOF18 mice. As epiblasts from such an early stage contain a very limited number of cells, the procedure of whole-genome profiling currently presents a number of challenges. Also, as *Oct4*-GFP positive EpiSCs are very similar to the parental EpiSCs based on microarray gene analysis (Figure 3C), we sought to compare the specific genes differentially expressed in *Oct4*-GFP positive and negative EpiSCs. To this end, *Oct4*-GFP positive cells from both E5.5 and E6.5 epiblasts were sorted and analyzed by real-time PCR. Genes that were differentially expressed in *Oct4*-GFP positive and negative EpiSCs (Figure 3A), such as *Rex1* (*Zfp42*), *Esrrb*, *Fbxo15*, *Klf2*, *Klf4*, *Klf5*, *Stella*, *Dppa4*, *Dppa5*, *Dnmt3l*, *Piwil2*, *Fragilis*, and *T*, were selected for analysis. Consistent with the microarray data, the majority of ESC markers were highly expressed in both *Oct4*-GFP positive EpiSCs and E5.5 epiblasts compared with *Oct4*-GFP negative EpiSCs and E6.5 epiblasts, respectively (Figures 5A and 5B). On the other hand, *Fragilis* and *T* were highly expressed in *Oct4*-GFP negative EpiSCs and E6.5 epiblasts compared with *Oct4*-GFP positive EpiSCs and E5.5 epiblasts, respectively (Figures 5A and 5B). Thus, the expression patterns of *Oct4*-GFP positive and negative EpiSCs correlate to those of E5.5 and E6.5 epiblasts, respectively. Next, we used computational analysis to determine the association between the EpiSC subpopulations and the in vivo epiblasts of different stages. The heat map calculated with the real-time RQ values again shows a very similar association (Figure 5C). Finally, the hierarchical clustering generated with the real-time PCR data clearly shows that *Oct4*-GFP positive EpiSCs are similar to E5.5 epiblasts, whereas *Oct4*-GFP negative EpiSCs rather represent E6.5 epiblasts (Figure S3).

Oct4 transcription is regulated through the DE in the ICM and ESCs but through the PE in the epiblast and EpiSCs (Tesar et al., 2007; Yeom et al., 1996). Using a luciferase assay, we compared *Oct4* enhancer utilization/activity in both *Oct4*-GFP positive and negative EpiSCs. As a control, we used ES-like cells that had been converted from *Oct4*-GFP positive EpiSCs. *Oct4*-GFP negative EpiSCs specifically used the PE, and the converted ES-like cells showed strong DE activity, as expected (Figure 5D). Although converted ES-like cells are maintained in the presence of 2i+LIF medium, spontaneous differentiation of the converted cells into EpiSCs could explain the residual PE activity observed. Accordingly, ESCs, which are derived directly from the ICM, showed exactly the same enhancer utilization as converted ES-like cells (data not shown). Of interest, *Oct4*-GFP positive EpiSCs preferentially utilize the PE, but they also exhibit some DE activity (Figure 5D). This unexpected DE activity in *Oct4*-GFP positive EpiSCs, although lower than PE activity, encouraged us to analyze the enhancer activity in early-stage in vivo epiblasts. We isolated in vivo epiblasts (E5.5, E6.6, and E7.5) from both GOF18 (containing DE and PE) and GOF18ΔPE mice. As mentioned above, in vivo epiblasts and their in vitro derivatives, EpiSCs, have been described to preferentially use the PE for *Oct4* transcription (Guo et al., 2009; Hanna et al., 2009; Tesar et al., 2007; Yeom et al., 1996). The in vivo epiblasts isolated from GOF18 mice on E5.5, E6.6, and E7.5 were GFP positive, as expected (Figure 5E). However, the in vivo GOF18ΔPE epiblasts (E5.5 and E6.5), which were supposed to be GFP negative due to the absence of PE, were also GFP positive, but GFP expression was clearly weaker than that in GOF18 mice—i.e., the GFP signals were barely detectable without overexposure, consistent with a previous report (Yoshimizu et al., 1999). GFP intensity had gradually decreased in E6.5, with GFP negative expression evident at E7.5, except for PGCs (Figure 5E). This observation strongly suggests that the early-stage epiblast still retains residual DE activity, together with PE activity. Thus, the enhancer switch, an event widely

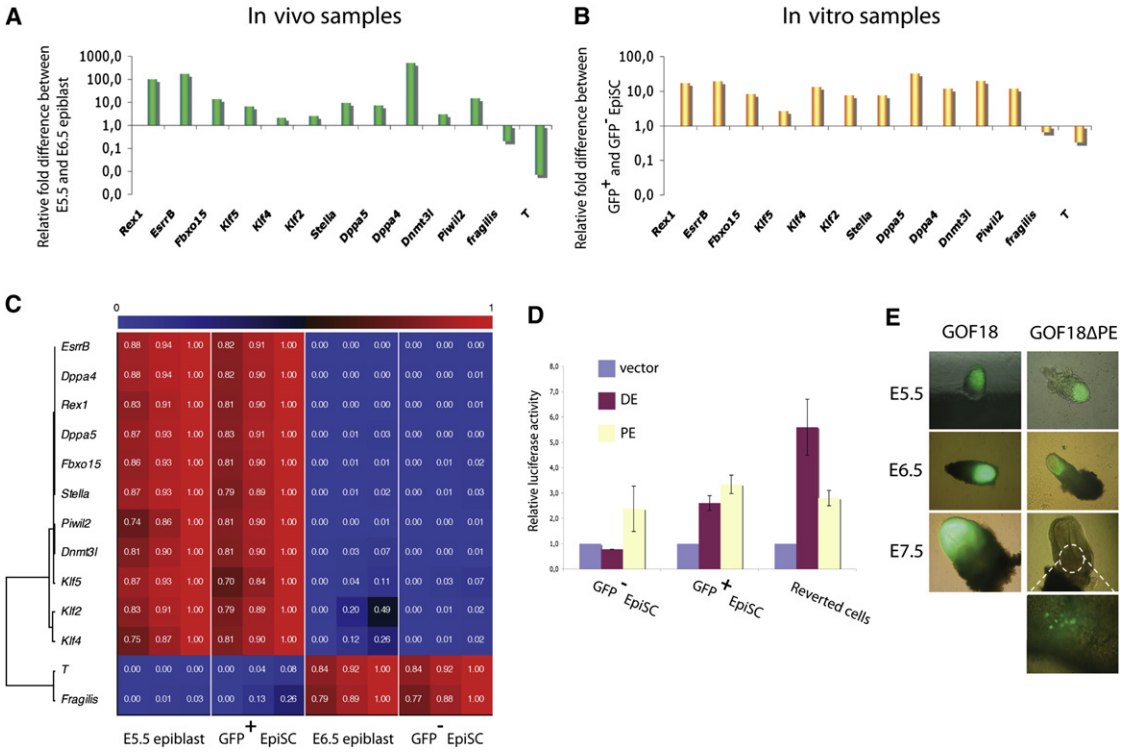

Figure 5. *Oct4*-GFP Positive and Negative EpiSCs Represent In Vivo Epiblasts of Different Developmental Stages

(A and B) Comparison of gene expression patterns in in vivo samples (E5.5 versus E6.5 epiblasts) (A) and in vitro samples (*Oct4*-GFP positive versus negative EpiSCs) (B). Expression levels are normalized to those of E6.5 epiblast (A) and *Oct4*-GFP negative EpiSCs (B), respectively.

(C) Heat map of the RT-PCR values. RT-PCR RQ ratios were used to compare in vivo with in vitro samples. The in vivo ratios were calculated by dividing the RT-PCR RQ value of the E6.5 epiblast by that of the E5.5 epiblast sample. The in vitro ratios were calculated by dividing the RT-PCR RQ value of the GFP negative EpiSC sample by that of the GFP positive EpiSC sample. The color bar at top codifies the ratio values; red and blue colors indicate high and low ratios, respectively.

(D) Evaluation of the *Oct4* enhancer activity in *Oct4*-GFP positive and negative EpiSCs. Relative luciferase activity was normalized to the activity of the empty vector. Data represent mean ± SEM of triplicates; n = 3.

(E) Dynamics of the *Oct4*-GFP reporter expression in in vivo epiblasts. In vivo epiblasts were isolated from both GOF18 and GOF18ΔPE mice at E5.5, 6.5, and 7.5. *Oct4*-GFP expression was measured under fluorescence microscope. To show specific *Oct4*-GFP expression from GOF18ΔPE mice, all images were taken with the same overexposure, but the images from GOF18 mice were taken with normal exposure. The extra panel under the E7.5 GOF18ΔPE epiblast shows residual *Oct4*-GFP expression in PGCs.

See also Figure S3.

accepted to occur around the time of implantation (E4.5), appears to occur later than expected. Therefore, the DE activity observed in *Oct4*-GFP positive EpiSCs also correlates with *Oct4* enhancer utilization in early-stage epiblasts (Figures 5D and 5E).

The enhancer utilization assay, combined with the real-time PCR data, suggests that *Oct4*-GFP positive EpiSCs correspond to an epiblast of an early developmental stage, whereas *Oct4*-GFP negative EpiSCs are rather similar to an epiblast of a later stage.

Oct4-GFP Positive EpiSCs Can Contribute to Chimeras

Gardner et al. reported that the PrE from E5 embryos is capable of contributing to chimera formation by blastocyst injection, unlike that from E6 and E7 embryos (Gardner et al., 1985). To determine whether there is a functional difference between *Oct4*-GFP positive and negative EpiSCs, just like between early- and late-stage in vivo epiblasts, we assessed whether these two cell populations can contribute to chimeras. Consistent with previous studies (Brons et al., 2007; Guo et al., 2009; Tesar et al., 2007), upon injection of *Oct4*-GFP positive EpiSCs into blastocysts, only ~10% of the embryos showed ICM integration (Figure 6A). Surprisingly, following transfer of these embryos, germline contribution as well as coat-color chimerism was noted (Figures 6B and 6C and Table S1). However, we were unable to observe any evidence of germline transmission with *Oct4*-GFP positive EpiSCs (Table S1). To trace the fate of *Oct4*-GFP negative EpiSCs in reconstructed embryos, we first infected GOF18 EpiSCs with a Td-tomato lentivirus. We then established a new Td-tomato GOF18 EpiSC line (Epi-Red) (Figure 6D). Tomato-positive/*Oct4*-GFP negative cells were FACS sorted and injected into blastocysts, but neither ICM integration (Figure 6E and Figure S4 available online) nor chimera contribution was observed (Table S1). Thus, *Oct4*-GFP negative EpiSCs, which made up

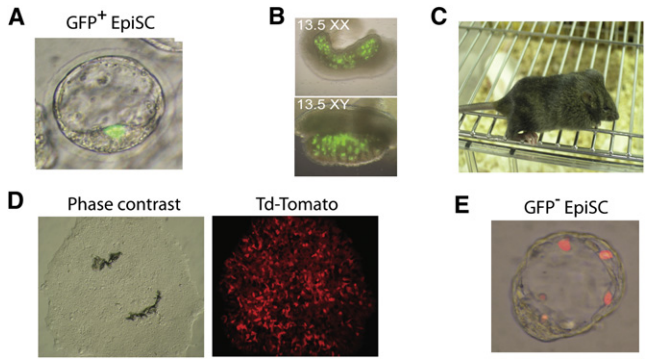

Figure 6. *Oct4*-GFP Positive EpiSCs Can Contribute to Chimera Formation

(A) Integration of *Oct4*-GFP positive EpiSCs into the ICM following blastocyst injection.

(B) Germline contribution of *Oct4*-GFP positive EpiSCs, as shown by the expression of *Oct4*-GFP in the gonad of a 13.5 days postcoitum (dpc) embryo.

(C) Coat-color chimera from *Oct4*-GFP positive EpiSCs.

(D) Morphology of Epi-Red cells and expression of Td-tomato lentivirus.

(E) Epi-Red cells failed to integrate into the ICM following blastocyst injection.

See also Figure S4.

~99% of the EpiSCs in culture, had no developmental potential, unlike *Oct4*-GFP positive EpiSCs.

Taken together, our data suggest that *Oct4*-GFP positive EpiSCs represent cells of an early-stage epiblast (E5.5), whereas *Oct4*-GFP negative EpiSCs are rather similar to those of a late-stage epiblast (E6.5 or E7.5).

Dppa5 Overexpression Increases the Early-Stage Epiblast Fraction

We have demonstrated that EpiSCs are heterogeneous and comprise two subpopulations—*Oct4*-GFP positive and negative cells, representing early- and late-stage epiblasts, respectively. Thus, we then tested whether overexpressing *Dppa5*, a gene that is specifically expressed in early-stage epiblasts and *Oct4*-GFP positive EpiSCs, but not in late-stage epiblasts and *Oct4*-GFP negative EpiSCs, can increase the *Oct4*-GFP positive fraction. *Dppa5*-overexpressing EpiSCs showed an ~6-fold increase in *Oct4*-GFP positive cells compared with noninfected EpiSCs (Figure 7A). We then FACS sorted the GFP positive cells from *Dppa5*-overexpressing and control EpiSCs and cultured them for another 10 passages (Figure 7B). *Oct4*-GFP positive cells from both *Dppa5*-overexpressing and control EpiSCs immediately started to lose *Oct4*-GFP expression. After two passages, 10.5% of the *Dppa5*-overexpressing cells and 6.3% of the control EpiSCs remained GFP positive. The number of GFP positive cells from control EpiSCs continued to decrease until levels reached those of the parental nonsorted EpiSCs—1.3% at passage 4. However, GFP positive cells were stably maintained in *Dppa5*-overexpressing EpiSCs at ~4%–6%, even after several passages. To exclude the possibility that *Dppa5* overexpression could revert EpiSCs to an ES-like state,

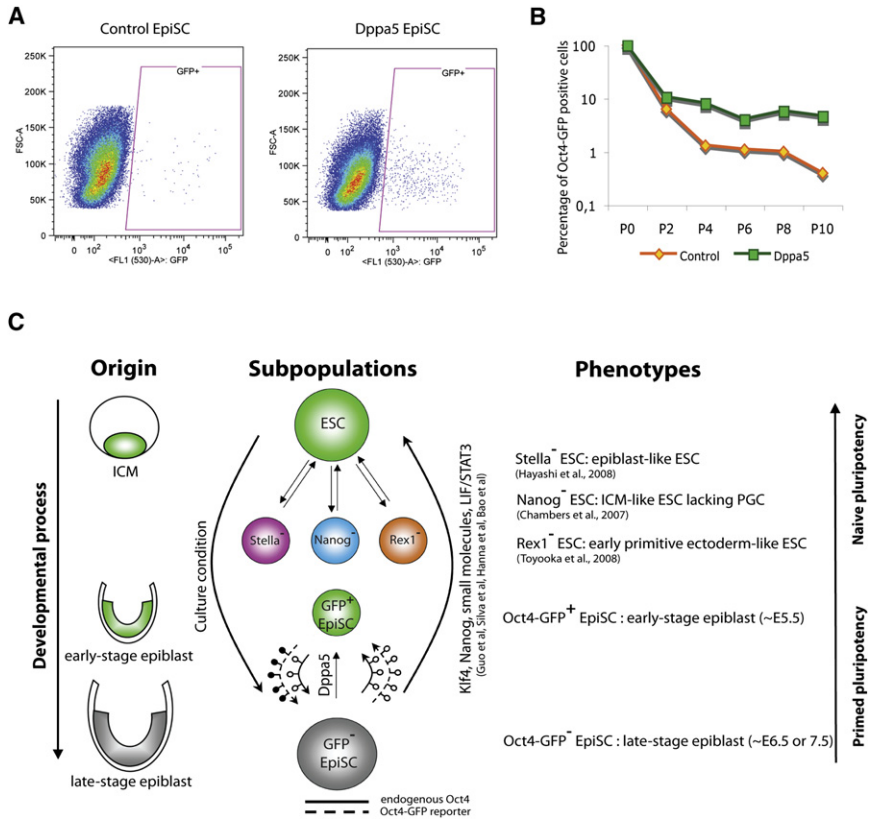

Figure 7. *Dppa5* Overexpression Increases the Early-Stage Epiblast Fraction

(A) The *Oct4*-GFP positive fraction was increased by overexpressing *Dppa5*. The numbers of *Oct4*-GFP positive cells from both control and *Dppa5*-overexpressing EpiSCs were compared by FACS.

(B) Dynamics of *Oct4*-GFP expression in FACS-sorted GFP positive cells from both control and *Dppa5*-overexpressing EpiSCs. FACS-sorted *Oct4*-GFP positive cells were cultured for another 10 passages, and the number of *Oct4*-GFP positive cells was measured after every two passages.

(C) A dynamic interchange exists between ESCs positive and negative for *Stella* (*Dppa3*), *Nanog*, and *Rex1* (*Zfp42*). When all three genes are expressed, ESCs represent the well-known ground state of pluripotency. However, when the expression of one of these genes is reduced, the pluripotent capability is also considerably reduced. EpiSCs are also heterogeneous, with two different populations distinguished by *Oct4*-GFP transgene expression. *Oct4*-GFP positive and negative EpiSCs exist in a state of dynamic equilibrium and correspond to in vivo epiblasts of early and late stages of development, respectively. The endogenous *Oct4* locus is unmethylated and expressed in both populations, whereas the *Oct4*-GFP transgene is differentially methylated, allowing to distinguish the early- and late-stage epiblast subpopulations.

See also Figure S2.

Oct4-GFP cells were sorted from *Dppa5*-overexpressing EpiSCs, and the methylation status of the *Rex1* promoter was assessed by bisulfite sequencing PCR. *Rex1* promoter was highly methylated, like in *Oct4*-GFP positive and negative EpiSCs, indicating that the increased *Oct4*-GFP positive fraction still maintains EpiSC identity rather than acquires an ES-like state (Figure S2). Therefore, these data suggest that overexpression of *Dppa5* increases the *Oct4*-GFP positive EpiSC fraction, which represents early-stage epiblasts.

DISCUSSION

The pluripotency of a cell can be assessed by determining the cell's developmental potential both in vitro and in vivo. The in vivo differentiation of cells to form both teratomas and chimeras is a basic yet reliable tool for assessing a cell's developing potency. Thus, cells that are pluripotent must meet these two basic criteria. EpiSCs, however, exhibit limited developing potency and thus have a unique pluripotential capacity compared with other pluripotent stem cell lines from different tissues of origin. The discrepancy in the potency of EpiSCs observed with different developmental assays, together with the heterogeneity of ESCs, prompted us to closely investigate the pluripotential state of EpiSCs. To this end, we assessed whether EpiSCs also exhibit heterogeneity, like ESCs. Our results show that EpiSCs are not as homogeneous as previously described (Hayashi et al., 2008; Toyooka et al., 2008). We have taken advantage of the differential expression of an *Oct4*-GFP transgene and have defined a novel type of EpiSCs. We found a dynamic interchange of two distinct cell subpopulations of EpiSCs that are in equilibrium in vitro: *Oct4*-GFP positive and *Oct4*-GFP negative EpiSCs (Figure 7C). We speculate that the distinct expression levels of the endogenous *Oct4* and the *Oct4*-GFP reporter result from an adaptation of the embryonal epiblast to culture conditions during the establishment of the EpiSCs, consistent with adaptive modifications described for ESCs (Buehr and Smith, 2003; Rossant, 2001). Nevertheless, using a luciferase assay, we showed that the two subpopulations exhibit distinct *Oct4* enhancer utilization. Therefore, although we discovered the existence of two types of EpiSCs—*Oct4*-GFP positive and negative EpiSC subpopulations—based on distinct transgene expression, this expression indeed represents distinct enhancer activity of the endogenous *Oct4* locus (Figures 5D and 5E).

Bao et al. recently showed the spontaneous conversion of EpiSCs to ES-like cells in ESC medium in the absence of exogenous transcription factors or small molecules (Bao et al., 2009). To investigate whether *Oct4*-GFP positive EpiSCs represent converted ES-like cells, we compared the distinctive features of EpiSCs and ESCs. First, the global gene expression profile of *Oct4*-GFP positive EpiSCs correlated with that of EpiSCs, but not with ESCs (Figures 3C and 3D). Second, as the promoter regions of *Stella* and *Rex1* were shown to be hypomethylated in ESCs but hypermethylated in EpiSCs (Bao et al., 2009; Hayashi et al., 2008), we examined the methylation of these two genes as a hallmark for discriminating EpiSCs from ESCs or converted ES-like cells. Consistent with these previous studies, both the *Stella* and *Rex1* promoters, as well as other germ cell marker gene promoters, were hypomethylated in ESCs but highly methylated in *Oct4*-GFP positive EpiSCs. In contrast, ES-like cells that had been converted from *Oct4*-GFP positive EpiSCs showed exactly the same DNA methylation pattern as ESCs. Third, we investigated the signaling dependence of these cells by comparing their *Oct4* enhancer utilization. We found that *Oct4*-GFP negative EpiSCs specifically use the PE, but converted ES-like cells and ESCs preferentially use the DE rather than the PE, as expected. Surprisingly, although *Oct4*-GFP positive EpiSCs mainly use the PE, a lower DE activity could also be detected, indicating that *Oct4*-GFP positive EpiSCs have a completely different pattern of *Oct4* enhancer utilization than ESCs. Taken together, these results show that *Oct4*-GFP positive EpiSCs are not converted ES-like cells.

We have also demonstrated that *Oct4*-GFP positive and negative EpiSCs correspond to developing epiblasts of two different stages. In terms of gene expression profile, *Oct4*-GFP positive EpiSCs correlate with E5.5 epiblasts and *Oct4*-GFP negative EpiSCs with E6.5 epiblasts. Moreover, *Oct4* enhancer utilization of *Oct4*-GFP positive EpiSCs resembles that of early epiblasts (~E5.5). Therefore, *Oct4*-GFP positive EpiSCs represent early-stage in vivo epiblast cells, whereas *Oct4*-GFP negative EpiSCs, the majority of EpiSCs, represent late-stage in vivo epiblast cells.

Finally, we compared the developmental potential of *Oct4*-GFP positive and negative EpiSCs. Although germline transmission could not be observed, *Oct4*-GFP positive EpiSCs could incorporate into the ICM and even contribute to the germline, unlike *Oct4*-GFP negative EpiSCs. PrE cells from E5 embryos retain the ability to give rise to adult chimeras, whereas PrE cells from E6 and E7 embryos have lost this ability (Gardner et al., 1985). Therefore, in terms of gene expression profile, epigenetic status, specific *Oct4* enhancer utilization, and even functional developmental capacity, *Oct4*-GFP positive and negative EpiSCs represent in vivo epiblasts of early and late developmental stages, respectively. EpiSCs rarely exhibit chimeric contribution, with the chimera rate (~0.5%) correlating with the percentage of *Oct4*-GFP positive cells in GOF18 EpiSCs (Brons et al., 2007). Thus, it is likely that the cells that contribute to chimera formation are the EpiSCs of an early in vivo epiblast—i.e., *Oct4*-GFP positive EpiSCs.

Taken together, our findings demonstrate that EpiSC cultures are heterogeneous and comprise *Oct4*-GFP positive and negative EpiSC cell subpopulations that are in a state of dynamic equilibrium and that correspond to in vivo epiblasts of early and late developmental stages, respectively (Figure 7C). Moreover, our data also suggest that the introduction of an early-stage-specific transcription factor, such as *Dppa5*, could increase the EpiSC subpopulation that represents early-stage epiblasts (Figures 7A and 7B). Therefore, investigations with EpiSCs derived from GOF18 mice offer opportunities to better understand early embryonic development, differentiation processes, and germ cell development, as well as the developing potency of in vivo epiblasts of different developmental stages. As EpiSCs have many properties in common with human ESCs, it would be interesting to assess whether human ESCs also exhibit heterogeneity, similar to EpiSCs, which may affect the therapeutic potential of these cells.

EXPERIMENTAL PROCEDURES

Cell Culture

The derivation and characterization of GOF18 EpiSCs is described elsewhere (Greber et al., 2010). In brief, E5.5 embryos (129/Sv female × C56/Bl6 and DBA/2 background GOF18+/+ male) were collected and transferred into HBSS medium. For dissection, deciduas were removed with forceps, and the extraembryonic ectoderm was separated from the epiblast by using hand-pulled glass pipettes. After washing with PBS, the epiblast was cultured on MEFs in EpiSC medium: DMEM/F12 (GIBCO BRL) containing 20% knockout serum replacement (GIBCO BRL), 2 mM glutamine, 1× nonessential amino acids, and 5 ng/ml bFGF. After initial culture on MEFs for three to five passages, EpiSC colonies were picked and transferred onto dishes that had been precoated with FCS for 30 min. Feeder-free EpiSCs were cultured in MEF (CF1 mice) conditioned medium. For conditioning, irradiated MEFs were seeded at a density of 5×10^4 cells/cm^2 and incubated in EpiSC medium for 24 hr. The conditioned medium was filtered, and bFGF (5 ng/ml) was added. For passaging feeder-free EpiSCs, colonies were incubated with collagenase IV (Invitrogen) for 5 min at 37°C and triturated by using a cell scraper. Cell clumps were replated on FCS-coated dishes, and the medium was changed every 24 hr.

DNA Methylation Analysis

DNA methylation status of EpiSCs was determined by the bisulfite sequencing method from our published protocol (Han et al., 2009). Detailed protocols, including PCR conditions and primer sequences, are described in our previous study (Han et al., 2008) and in the Extended Experimental Procedures.

Whole-Genome Expression Analysis

Global gene expression profiling was performed with the Illumina microarray. Detailed protocols are described in the Extended Experimental Procedures.

Blastocyst Injection

Blastocysts were collected from B6C3F1 mice. EpiSCs were recovered by treatment with collagenase IV or 0.25% trypsin EDTA, and 10–15 cells were loaded into an injection pipette and injected into B6C3F1 blastocysts by Piezo (Prime-tech). Each of the 15 injected blastocysts was transferred into the uterus of a pseudopregnant ICR mouse.

SUPPLEMENTAL INFORMATION

Supplemental Information includes Extended Experimental Procedures, four figures, and one table and can be found with this article online at doi: 10.1016/j.cell.2010.10.015.

ACKNOWLEDGMENTS

We are indebted to all members of the Schöler laboratory for fruitful discussions on the results. We are especially grateful to Dr. Paul Tesar for providing the T9 EpiSC line. We are also grateful to Göran Key, Inge Sobek-Klocke, Martina Sinn, and David Obridge for technical assistance and Areti Malapetsas for editing the manuscript. This work was supported by the Federal Ministry of Education and Research (BMBF) initiative "Cell-Based Regenerative Medicine" (Grant 01GN0539).

Received: April 9, 2010
Revised: August 17, 2010
Accepted: October 12, 2010
Published online: November 4, 2010

REFERENCES

Bao, S., Tang, F., Li, X., Hayashi, K., Gillich, A., Lao, K., and Surani, M.A. (2009). Epigenetic reversion of post-implantation epiblast to pluripotent embryonic stem cells. Nature *461*, 1292–1295.

Brons, I.G., Smithers, L.E., Trotter, M.W., Rugg-Gunn, P., Sun, B., Chuva de Sousa Lopes, S.M., Howlett, S.K., Clarkson, A., Ahrlund-Richter, L., Pedersen, R.A., and Vallier, L. (2007). Derivation of pluripotent epiblast stem cells from mammalian embryos. Nature *448*, 191–195.

Buehr, M., and Smith, A. (2003). Genesis of embryonic stem cells. Philos. Trans. R. Soc. Lond. B Biol. Sci. *358*, 1397–1402, discussion 1402.

Carter, M.G., Stagg, C.A., Falco, G., Yoshikawa, T., Bassey, U.C., Aiba, K., Sharova, L.V., Shaik, N., and Ko, M.S. (2008). An in situ hybridization-based screen for heterogeneously expressed genes in mouse ES cells. Gene Expr. Patterns *8*, 181–198.

Chambers, I., Silva, J., Colby, D., Nichols, J., Nijmeijer, B., Robertson, M., Vrana, J., Jones, K., Grotewold, L., and Smith, A. (2007). Nanog safeguards pluripotency and mediates germline development. Nature *450*, 1230–1234.

Chou, Y.F., Chen, H.H., Eijpe, M., Yabuuchi, A., Chenoweth, J.G., Tesar, P., Lu, J., McKay, R.D., and Geijsen, N. (2008). The growth factor environment defines distinct pluripotent ground states in novel blastocyst-derived stem cells. Cell *135*, 449–461.

Furusawa, T., Ohkoshi, K., Honda, C., Takahashi, S., and Tokunaga, T. (2004). Embryonic stem cells expressing both platelet endothelial cell adhesion molecule-1 and stage-specific embryonic antigen-1 differentiate predominantly into epiblast cells in a chimeric embryo. Biol. Reprod. *70*, 1452–1457.

Gardner, R.L., Lyon, M.F., Evans, E.P., and Burtenshaw, M.D. (1985). Clonal analysis of X-chromosome inactivation and the origin of the germ line in the mouse embryo. J. Embryol. Exp. Morphol. *88*, 349–363.

Greber, B., Wu, G., Bernemann, C., Joo, J.Y., Han, D.W., Ko, K., Tapia, N., Sabour, D., Sterneckert, J., Tesar, P., and Schöler, H.R. (2010). Conserved and divergent roles of FGF signaling in mouse epiblast stem cells and human embryonic stem cells. Cell Stem Cell *6*, 215–226.

Guo, G., Yang, J., Nichols, J., Hall, J.S., Eyres, I., Mansfield, W., and Smith, A. (2009). Klf4 reverts developmentally programmed restriction of ground state pluripotency. Development *136*, 1063–1069.

Han, D.W., Do, J.T., Gentile, L., Stehling, M., Lee, H.T., and Schöler, H.R. (2008). Pluripotential reprogramming of the somatic genome in hybrid cells occurs with the first cell cycle. Stem Cells *26*, 445–454.

Han, D.W., Do, J.T., Araúzo-Bravo, M.J., Lee, S.H., Meissner, A., Lee, H.T., Jaenisch, R., and Schöler, H.R. (2009). Epigenetic hierarchy governing Nestin expression. Stem Cells *27*, 1088–1097.

Hanna, J., Markoulaki, S., Mitalipova, M., Cheng, A.W., Cassady, J.P., Staerk, J., Carey, B.W., Lengner, C.J., Foreman, R., Love, J., et al. (2009). Metastable pluripotent states in NOD-mouse-derived ESCs. Cell Stem Cell *4*, 513–524.

Hayashi, K., Lopes, S.M., Tang, F., and Surani, M.A. (2008). Dynamic equilibrium and heterogeneity of mouse pluripotent stem cells with distinct functional and epigenetic states. Cell Stem Cell *3*, 391–401.

Lawson, K.A., Meneses, J.J., and Pedersen, R.A. (1991). Clonal analysis of epiblast fate during germ layer formation in the mouse embryo. Development *113*, 891–911.

Lovell-Badge, R. (2007). Many ways to pluripotency. Nat. Biotechnol. *25*, 1114–1116.

Rivera-Pérez, J.A., and Magnuson, T. (2005). Primitive streak formation in mice is preceded by localized activation of Brachyury and Wnt3. Dev. Biol. *288*, 363–371.

Rossant, J. (2001). Stem cells from the Mammalian blastocyst. Stem Cells *19*, 477–482.

Silva, J., Nichols, J., Theunissen, T.W., Guo, G., van Oosten, A.L., Barrandon, O., Wray, J., Yamanaka, S., Chambers, I., and Smith, A. (2009). Nanog is the gateway to the pluripotent ground state. Cell *138*, 722–737.

Tesar, P.J., Chenoweth, J.G., Brook, F.A., Davies, T.J., Evans, E.P., Mack, D.L., Gardner, R.L., and McKay, R.D. (2007). New cell lines from mouse epiblast share defining features with human embryonic stem cells. Nature *448*, 196–199.

Toyooka, Y., Shimosato, D., Murakami, K., Takahashi, K., and Niwa, H. (2008). Identification and characterization of subpopulations in undifferentiated ES cell culture. Development *135*, 909–918.

Western, P., Maldonado-Saldivia, J., van den Bergen, J., Hajkova, P., Saitou, M., Barton, S., and Surani, M.A. (2005). Analysis of Esg1 expression in pluripotent cells and the germline reveals similarities with Oct4 and Sox2 and differences between human pluripotent cell lines. Stem Cells *23*, 1436–1442.

Yeom, Y.I., Fuhrmann, G., Ovitt, C.E., Brehm, A., Ohbo, K., Gross, M., Hübner, K., and Schöler, H.R. (1996). Germline regulatory element of Oct-4 specific for the totipotent cycle of embryonal cells. Development *122*, 881–894.

Ying, Q.L., Nichols, J., Chambers, I., and Smith, A. (2003). BMP induction of Id proteins suppresses differentiation and sustains embryonic stem cell self-renewal in collaboration with STAT3. Cell *115*, 281–292.

Yoshimizu, T., Sugiyama, N., De Felice, M., Yeom, Y.I., Ohbo, K., Masuko, K., Obinata, M., Abe, K., Schöler, H.R., and Matsui, Y. (1999). Germline-specific expression of the Oct-4/green fluorescent protein (GFP) transgene in mice. Dev. Growth Differ. *41*, 675–684.